Control of Asymmetric Magnetic Perturbations in Tokamaks

Jong-kyu Park,[1] Michael J. Schaffer,[2] Jonathan E. Menard,[1] and Allen H. Boozer[3]

[1]Princeton Plasma Physics Laboratory, Princeton, New Jersey 08543, USA

[2]General Atomics, San Diego, California 92186, USA

[3]Department of Applied Physics and Applied Mathematics, Columbia University, New York, New York 10027, USA

(Received 5 May 2007; published 9 November 2007)

The sensitivity of tokamak plasmas to very small deviations from the axisymmetry of the magnetic field $|\delta\vec{B}/\vec{B}| \approx 10^{-4}$ is well known. What was not understood until very recently is the importance of the perturbation to the plasma equilibrium in assessing the effects of externally produced asymmetries in the magnetic field, even far from a stability limit. DIII-D and NSTX experiments find that when the deleterious effects of asymmetries are mitigated, the external asymmetric field was often made stronger and had an increased interaction with the magnetic field of the unperturbed equilibrium. This Letter explains these counterintuitive results. The explanation using ideal perturbed equilibria has important implications for the control of field errors in all toroidal plasmas.

DOI: 10.1103/PhysRevLett.99.195003 PACS numbers: 52.55.Fa, 52.30.Cv, 52.55.Tn

The best plasma confinement using magnetic fields is obtained in tokamaks, and the burning plasma experiment ITER [1] will be a tokamak. A tokamak is nominally axisymmetric, and its performance can be greatly degraded by small externally produced magnetic fields that break the symmetry [2–7]. Asymmetries, such as imperfections in the primary magnets, can be important even when the ratio of the externally produced magnetic perturbation $\vec{b}^x$ to the equilibrium magnetic field $\vec{B}$ satisfies $|\vec{b}^x|/|\vec{B}| \approx 10^{-4}$. At a sufficient amplitude, $\vec{b}^x$ stops plasma rotation, called mode locking [2–5], which often results in a catastrophic destruction of the plasma equilibrium, called a disruption.

Here it is shown that paradoxes that have arisen between previous theoretical suppositions and mode locking experiments are resolved by the new ideal perturbed equilibrium code (IPEC) [8], the first computation of three-dimensionally perturbed tokamak plasma equilibria in high resolution. The results show that standard suppositions are incorrect on the response of plasmas to magnetic perturbations. The plasma response was known to be important near a stability limit [9], but we find that response greatly changes the perturbed state from the previous suppositions, even far from a stability limit. This new understanding appears to be an essential element in the establishment of tolerances for symmetry breaking in experiments, as ITER, as well as for finding ways to achieve these tolerances.

Mode locking occurs when the externally produced asymmetric field $\vec{b}^x$ exceeds a critical magnitude and is interpreted as the abrupt opening of a magnetic island on a rational surface. On rational surfaces, the magnetic field lines close after m toroidal and n poloidal circuits. The ratio of toroidal to poloidal circuits is the safety factor q; on a rational surface $q = m/n$. In the presence of a resonant field normal to the surface $(\vec{b}\cdot\hat{n})_{mn}$, a rational surface splits to form a magnetic island. If the plasma had zero resistivity, a surface current would arise to cancel the $(\vec{b}\cdot\hat{n})_{mn}$ driven by the external perturbation $\vec{b}^x$. These shielding surface currents can be sustained against resistivity by removing energy from plasma rotation when the driven $(\vec{b}\cdot\hat{n})_{mn}$ is less than a critical magnitude. When the shielding current is sustained, the plasma response remains effectively ideal and can be described accurately by ideal perturbed equilibria. For larger values, the shielding current is dissipated and the plasma flow becomes locked to the resulting island.

In an experiment, the externally produced asymmetric field $\vec{b}^x$ is the sum of fields from intrinsic imperfections in the device and a limited number of external control coils (Fig. 1). The only adjustable parameters are the currents in

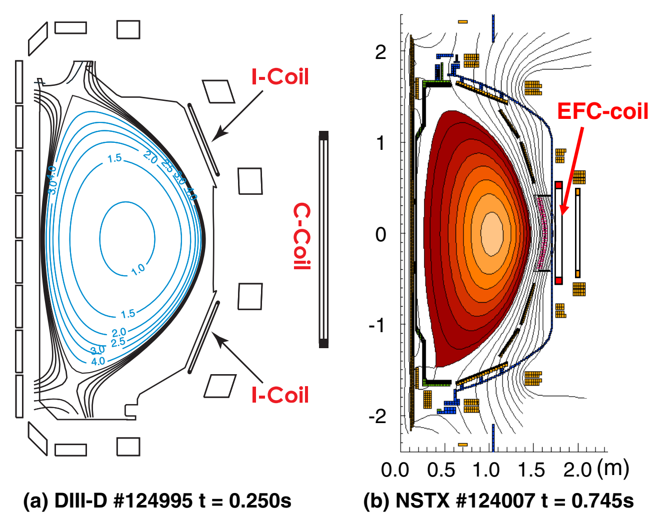

FIG. 1 (color online). The correction coils in (a) DIII-D (C coils and I coils) and (b) NSTX (EFC coils). The typical shapes of the axisymmetric equilibria in this study are also shown for each tokamak.

these control coils, which are too few to eliminate the $\vec{b}^x$ due to intrinsic imperfections. The number of $\vec{b}^x \cdot \hat{n}$ distributions of normal magnetic field on the plasma surface that can be adjusted is no more than the number of independent control coil currents. An important practical issue is how these currents are to be chosen to optimally mitigate the plasma effects of the intrinsic imperfections. A number of experiments have found the critical amplitude of the external field for mode locking is proportional to the plasma density, $(\vec{b}^x \cdot \hat{n})_c \propto n_L$. Therefore, the control coil currents can be empirically optimized by finding the currents for which the locking density n_L is minimized.

A long-standing supposition, which is supported by cylindrical theory [10,11], is that the resonant field driving the opening of islands, or the total resonant field, $(\vec{b} \cdot \hat{n})_{mn}$, is proportional to the resonant component of the external field, or external resonant field, $(\vec{b}^x \cdot \hat{n})_{mn}$. The external resonant field is a vacuum field on a rational surface. When this supposition is applied to mode locking experiments on DIII-D [12] and NSTX [13], the results are paradoxical. When the control coil currents were optimized empirically, the external resonant field was often increased—not decreased as the standard supposition required. This implies that the total resonant field is very different from the external resonant field through perturbed and poloidally coupled plasma currents.

IPEC calculates perturbed equilibria with the shielding currents on rational surfaces and resolves the paradoxes by showing the total resonant field, the $(\vec{b} \cdot \hat{n})_{mn}$, are reduced when the control coil currents are adjusted empirically. IPEC also finds the amplitude of the $(\vec{b} \cdot \hat{n})_{mn}$ can be far more sensitive to the nonresonant than to the resonant harmonics in the external fields, the $(\vec{b}^x \cdot \hat{n})_{mn}$. These results differ fundamentally from standard views on the interaction with plasmas of magnetic asymmetries.

The DCON ideal magnetohydrodynamics stability code [14] was modified and augmented in IPEC to calculate perturbed equilibria. The perturbed force balance equations are solved to find the displacements $\vec{\xi}(\vec{x})$ of the magnetic field lines in a plasma due to a displacement of its boundary, $\vec{\xi} \cdot \hat{n}_b \equiv (\vec{\xi} \cdot \hat{n})(\psi = \psi_b, \theta, \varphi)$ at $\psi = \psi_b$, where $\hat{n}_b$ is the unit vector normal to the plasma boundary, θ is poloidal, and φ is a toroidal angle in any straight-field line, or flux, coordinates. The externally produced normal magnetic fields on the plasma boundary that are needed to produce the displacement $\vec{\xi} \cdot \hat{n}_b$ and the associated $\vec{b} = \vec{\nabla} \times (\vec{\xi} \times \vec{B})$ are found by placing a fictitious control surface infinitesimally outside the plasma. The normal component of $\vec{b}$ must be continuous and determines a unique curl-free magnetic field, $\vec{b}^v$, in the region outside the control surface. The tangential field has a discontinuity across the control surface, which determines a surface current $\vec{K}$ on that surface, $\mu_0 \vec{K} = [\hat{n}_b \times \vec{b}] \equiv \hat{n}_b \times \vec{b}^v - \hat{n}_b \times \vec{b}$. The normal magnetic field $\vec{b}^x \cdot \hat{n}_b$ produced by $\vec{K}$ is the normal component of the externally produced field required to sustain the displacement of the plasma boundary $\vec{\xi} \cdot \hat{n}_b$.

Each perturbed equilibrium is defined by the total magnetic perturbation normal to the plasma boundary, $(\vec{b}_i \cdot \hat{n}_b)$, and is also defined by the external magnetic field $(\vec{b}_i^x \cdot \hat{n}_b)$ required to produce it, as found using the control surface. With a sufficient number of perturbed equilibria, IPEC constructs [8] the linear permeability operator $\overleftrightarrow{P}$,

$$\vec{b} \cdot \hat{n}_b = \overleftrightarrow{P}[\vec{b}^x \cdot \hat{n}_b]. \tag{1}$$

Given an external error field on the boundary, $\overleftrightarrow{P}$ determines the total field on the boundary from which the DCON code can determine the perturbed plasma equilibrium. Figure 2 shows the examples of $n = 1$ displacements by intrinsic error fields in DIII-D and NSTX.

The shielding current at each rational surface $\vec{j}_s$ is given by the jump in the tangential magnetic field. In IPEC, this shielding current is calculated using [15]

$$\vec{j}_s = \frac{\Delta_{mn} m i e^{i(m\theta - n\varphi)}}{\mu_0 n^2 (\oint dS B^2 / |\vec{\nabla}\psi|^3)} \delta(\psi - \psi_{mn}) \vec{B}, \tag{2}$$

where the dimensionless quantity

$$\Delta_{mn} \equiv \left[\frac{\partial}{\partial \psi} \frac{\vec{b} \cdot \vec{\nabla}\psi}{\vec{B} \cdot \vec{\nabla}\varphi} \right]_{mn}. \tag{3}$$

The total resonant field, $(\vec{b} \cdot \hat{n})_{mn}$, which is the critical parameter for mode locking, is within a sign the field produced by the singular current, $\vec{\nabla} \times \vec{b} = \mu_0 \vec{j}_s$, and is calculated by IPEC.

The currents in the C coils and I coils [Fig. 1(a)] [5] of DIII-D have been used over a decade to minimize the effects of the dominant $n = 1$ intrinsic error field. Success is measured by a lowered locking density n_L. The typical test plasmas in DIII-D had a toroidal field at the magnetic axis, $B_{T0} = 1.0T$, a central $q_0 = 0.95$, an

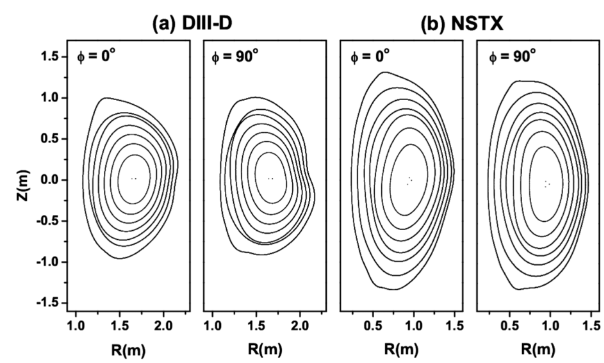

FIG. 2. The perturbed flux surfaces of (a) DIII-D and (b) NSTX target plasmas by each dominant $n = 1$ intrinsic error field. The amplitude of the perturbation for each figure is 15 times greater than the perturbation in each machine.

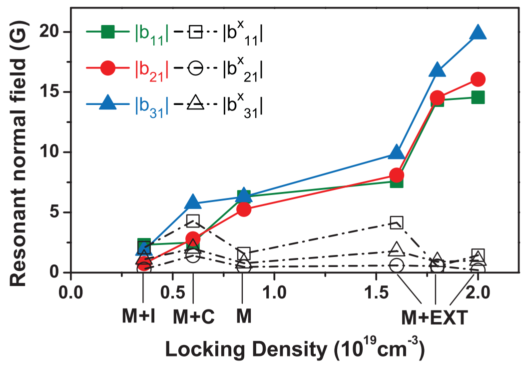

FIG. 3 (color). The total $|b_{m1}|$ and external $|b^x_{m1}|$, $m = 1, 2, 3$ resonant fields versus locking densities in each finalized case: machine intrinsic field (M), C coil ($M + C$), and I coil ($M + I$) optimized fields, and several external field correcting ($M +$ EFC) fields. Note the linear correlations and the amplifications in the total resonant fields compared with the external resonant fields.

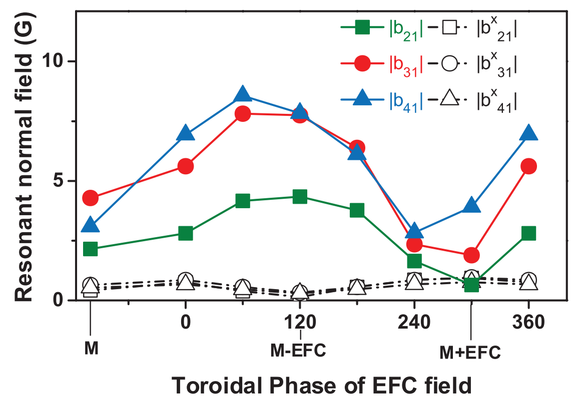

FIG. 4 (color). The variation of total $|b_{m1}|$ and external $|b^x_{m1}|$, $m = 1, 2, 3$, resonant fields versus the toroidal phase of the EFC-correcting field. Note opposite predictions and good consistency with the total resonant fields for the best and worst phases.

edge $q_{99} = 4.3$, and an aspect ratio $A = 2.7$, which is the ratio of major to minor radii of the toroidal plasma. These experiments yielded paradoxical results, which are summarized in Fig. 3. The various precalculated corrections of the external resonant field ($M +$ ext) actually increase locking densities, so C coils ($M + C$) and I coils ($M + I$) were optimized empirically to reduce locking density compared with only intrinsic error field (M). However, none of these finalized cases shows a proper correlation between locking densities and the external resonant fields $|b^x_{m1}| \equiv |(\vec{b}^x \cdot \hat{n})_{m,n=1}|$. The locking density is reduced even with large overcorrections of the external field as seen in the $M + C$ case. All these paradoxical results are resolved when calculating the total resonant field driving the island $|b_{m1}| \equiv |(\vec{b} \cdot \hat{n})_{m,n=1}|$, and the expected linear dependence on locking density n_L is seen as in Fig. 3. The experimental observation of a linear correlation between the $|b^x_{m1}|$ and n_L is misleading since this trend is true only when an external field distribution is fixed. It should also be noted that the actual drive for the islands, the $|b_{mn}|$ produced by the Δ_{mn}, are much larger than the external resonant field.

NSTX has found similar paradoxes in error field experiments. In NSTX, there are three pairs of error field control (EFC) coils, similar to the C coils of DIII-D, as shown in Fig. 1(b). The target plasmas have fixed $\bar{n} = 0.4 \times 10^{19}\ \mathrm{m}^{-3}$, $B_{T0} = 0.45$ T, $q_0 = 1.3$, $q_{99} = 11.2$, and $A = 1.5$. For the dominant $n = 1$ error field, there are only 2 degrees of freedom in the control coils: the amplitude and the toroidal phase of the $n = 1$ correction field. Despite this limitation of the error field control in NSTX, the EFC coils have given robust results for the best ($M +$ EFC), $\phi = 300$, and the worst phase ($M -$ EFC), $\phi = 120$, for locked modes [7]. Figure 4 shows the external resonant field $|b^x_{m1}|$ as well as the total resonant field, the $|b_{m1}|$, versus the toroidal phase of the error correction coil. Again the $|b^x_{m1}|$ are not correlated, or rather anticorrelated, with the mitigation of error field effects, but the $|b_{m1}|$ are well correlated.

The physics is clarified by the coupling coefficients between the various Fourier harmonics of the external field at the plasma boundary, the $|(\vec{b}^x \cdot \hat{n}_b)_{m,n=1}|$, and the total resonant field at a rational surface, which is proportional to $|\Delta_{m1}|$. Here Hamada [16] coordinates are chosen to define Fourier harmonics and the $q = 2/1$ surface is analyzed, but other flux coordinates and rational surfaces occupying the main volume of plasma led to a similar conclusion. For DIII-D, this coupling is given in Fig. 5(a), which shows the dominant coupling to $|\Delta_{21}|$ is from the $m = 7, 8, 9$ harmonics of the external field. Figure 5(b) shows the various external field harmonics, without, M, and with, $M + C$ and $M + I$, error field mitigation. Optimal error field mitigation with the C coils and the I coils was associated with similar reductions in the amplitudes of the external field harmonics, $m = 7, 8, 9$, that had the strongest coupling to

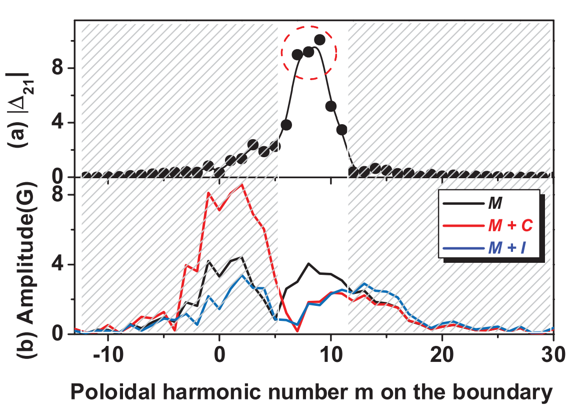

FIG. 5 (color). (a) The poloidal harmonic coupling spectrum for $|\Delta_{21}|$ and (b) the Fourier components of the external error field on the plasma boundary in DIII-D for machine intrinsic (M) and two optimized fields, ($M + C$) and ($M + I$). The dotted circle in (a) shows the most important harmonics of the external field.

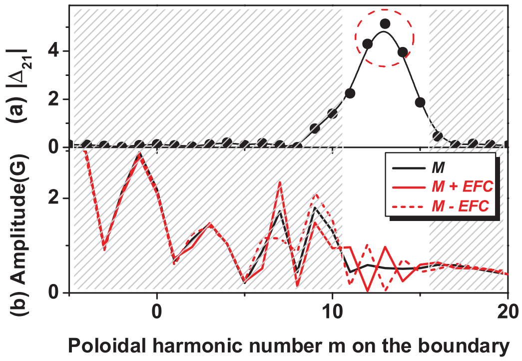

FIG. 6 (color). (a) The poloidal harmonic coupling spectrum for $|\Delta_{21}|$ and (b) the Fourier components of the external error field on the plasma boundary in NSTX for machine intrinsic (M), the best (M + EFC), and the worst (M − EFC) fields. The dotted circle in (a) shows the most important harmonics of the external field.

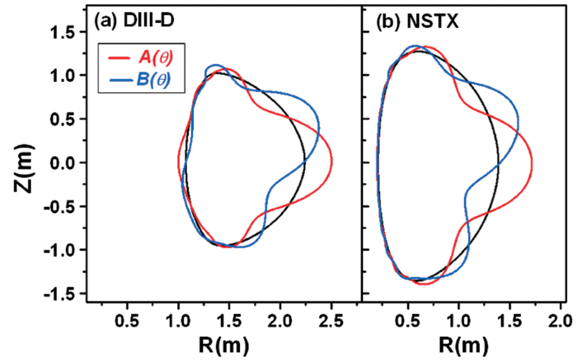

FIG. 7 (color). The distributions of the external field on the plasma boundary maximizing the total resonant fields on rational surfaces, for (a) DIII-D and (b) NSTX. The three-dimensional distribution can be constructed by $\vec{b}^x \cdot \hat{n}_b = A(\theta)\cos(\phi) + B(\theta) \times \sin(\phi)$ relative to the plasma boundary (black line).

$|\Delta_{21}|$. Although the C coil greatly enhanced the low harmonics of the external field when the $m = 7, 8, 9$ harmonics were reduced, this did not prevent a successful mitigation of error field effects. For NSTX the dominant coupling is from the $m = 12, 13, 14$ harmonics [Fig. 6(a)]. Indeed, two out of three of these harmonics are reduced when error field effects are mitigated (M + EFC), but two out of three are increased when error field effects are enhanced (M − EFC) by changing the toroidal phase of the EFC coil currents [Fig. 6(b)]. The large shift of the dominant poloidal harmonics to higher modes in both machines is the typical characteristic of the toroidal plasma response. Note that the test plasmas in both machines were stable and far from a stability limit.

The description of the external error field in terms of its Fourier harmonics on the plasma surface offers little insight since such high harmonics in flux coordinates are not easily controlled in real space. Much better insight is obtained from the distribution on the plasma surface of the normal component of the external field that maximizes the total resonant fields. This distribution can be written as $\vec{b}^x \cdot \hat{n}_b = A(\theta)\cos(\phi) + B(\theta)\sin(\phi)$, where ϕ is the polar toroidal angle. Figure 7 represents these two functions as a deviation from a surface that represents the plasma edge for DIII-D [Fig. 7(a)] and NSTX [Fig. 7(b)]. Figure 7 implies that the asymmetric variation in external field on the outboard side is most important and should be controlled. The dominant patterns are weakly dependent on target plasmas and explains the successful cancellation of error fields by the C coils in DIII-D and EFC coils in NSTX, despite their limitations in the control of poloidal distribution.

In summary, a comparison of theory and experiment has shown that magnetic perturbations that drive islands on low order rational magnetic surfaces in tokamaks are greatly modified by the perturbation to the plasma equilibrium. The plasma is far more sensitive to particular components (Figs. 5 and 6) or distributions (Fig. 7) of the external normal field on the plasma boundary, $\vec{b}^x \cdot \hat{n}_b$. The effects of field errors can be mitigated by controlling the currents in external coils to null the drive of these distributions, as verified in locking experiments.

Special thanks to Alan H. Glasser and Morrell S. Chance for assistance. This work was supported by DOE Contracts No. DE-AC02-76CH03073 (PPPL), No. DE-FC02-04ER54698 (GA), and No. DE-FG02-03ERS496 (CU).

[1] K. Ikeda, Nucl. Fusion **47**, S1 (2007).
[2] T. C. Hender *et al.*, Nucl. Fusion **32**, 2091 (1992).
[3] R. J. La Haye, R. Fitzpatrick, T. C. Hender, A. W. Morris, J. T. Scoville, and T. N. Todd, Phys. Fluids B **4**, 2098 (1992).
[4] R. J. Buttery *et al.*, Nucl. Fusion **39**, 1827 (1999).
[5] J. T. Scoville and R. J. LaHaye, Nucl. Fusion **43**, 250 (2003).
[6] J. E. Menard *et al.*, Nucl. Fusion **43**, 330 (2003).
[7] M. G. Bell *et al.*, Nucl. Fusion **46**, S565 (2006).
[8] J.-K. Park, A. H. Boozer, and A. H. Glasser, Phys. Plasmas **14**, 052110 (2007).
[9] A. H. Boozer, Phys. Rev. Lett. **86**, 5059 (2001).
[10] R. Fitzpatrick, Nucl. Fusion **33**, 1049 (1993).
[11] R. Fitzpatrick, Phys. Plasmas **5**, 3325 (1998).
[12] J. L. Luxon and L. G. Davis, Fusion Technol. **8**, 441 (1985).
[13] J. Spitzer, M. Ono, M. Peng, D. Bashore, T. Bigelow, A. Brooks, J. Chrzanowski, H. M. Fan, P. Heitzenroeder, and T. Jarboe, Fusion Technol. **30**, 1337 (1996).
[14] A. H. Glasser and M. S. Chance, Bull. Am. Phys. Soc. **42**, 1848 (1997).
[15] A. H. Boozer and C. Nührenberg, Phys. Plasmas **13**, 102501 (2006).
[16] S. Hamada, Nucl. Fusion **2**, 23 (1962).